Electronic Supplementary Information (ESI)

Rational Design and Synthesis of a Porous, Task-Specific Polycarbazole for Efficient CO_2 Capture

Tian Jin,[a,†] Yan Xiong,[a,†] Xiang Zhu,[*,b] Ziqi Tian,[c] Duan-Jian Tao,[b] Jun Hu,[a] De-en Jiang,[c] Hualin Wang,[d] Honglai Liu[*,a] and Sheng Dai[*,b]

[a]*State Key Laboratory of Chemical Engineering and Department of Chemistry, East China University of Science and Technology, Shanghai, 200237, P. R. China.*

Email: ***hlliu@ecust.edu.cn***

[b]*Department of Chemistry, The University of Tennessee, Knoxville, Tennessee 37996-1600, United States.*

Email: ***xiang@utk.edu (zhuxiang.ecust@gmail.com)***,

dais@ornl.gov.

[c] *Department of Chemistry, University of California, Riverside, CA 92521, United States*

[d] *State Environmental Protection Key Laboratory of Environmental Risk Assessment and Control on Chemical Process, East China University of Science and Technology, Shanghai 200237, China*

[†] *These authors contributed equally.*

Chemicals:

All commercially available solvents and other chemicals were purchased from local suppliers and used without further purification. 3,5,6-tetrafluoropyridine (96 %) was obtained from TCI. Carbazole (98 %) was purchased from Adamas reagent Co., Ltd. Potassium carbonate (99 %) was obtained from Shanghai Lingfeng Chemistry Reagents Co., Ltd. Anhydrous ferric chloride (97 %) was purchased from Sinopharm Chemical Reagent Co., Ltd.

Material characterization: The morphology of the sample was characterized by using a JEOL JEM-2100 transmission electron microscopy (TEM). The powder X-ray diffraction (PXRD) data were carried out on a D/Max2550 VB/PC diffractometer (40 kV, 200 mA) using a Cu Kα as the radiation. The FT-IR spectra were recorded on a Nicolet iS10 FTIR spectrometer using the KBr pellet technique. Gas adsorption/desorption isotherm was measured by volumetric adsorption analyzer ASAP 2020 after the sample was degassed at 150 °C for 12 h under vacuum. Brunauer-Emmett-Teller (BET) and t-plot model were used to determine the specific surface area and t-plot micropore area of the samples, respectively. The total pore volume of the sample was estimated at a relative pressure of $P/P_0 = 0.99$. Pore size distributions (PSD) was calculated using nonlocal density functional theory (NLDFT). CO_2 adsorption isotherm was measured up to 1 atm at 273 and 298 K. The thermal decomposition behavior of the sample was performed on a NETZSCH STA 499 F3 thermogravimetric analyzer, and the sample was heated at a rate of 10 $^oC\ min^{-1}$ under N_2 gas flow at a rate of 40 mL min^{-1}. Elemental analysis was conducted on an elemental analyzer (Vario EL III). Solution ^1H nuclear magnetic resonance (NMR) spectrum was obtained in a $CDCl_3$ solution with a Bruker 400MHz Advance spectrometer. Solid state ^{13}C cross-polarization (CP)/magic-angle spinning (MAS) NMR spectrum was recorded with a Bruker Avance III- 600MHz spectrometer at a frequency of 100.62 MHz with 13 kHz spinning rate, and 1024 scans were signal averaged. The chemical shifts of ^{13}C NMR spectra were referenced to tetramethylsilane. Water contact angle measurement was carried out on JC2000D optical contact angle meter at ambient conditions.

CO_2/N_2 Uptake

CO_2 and N_2 adsorption isotherms of samples were measured using a Micromeritics ASAP 2020 static volumetric analyzer at two different temperatures 273 and 298 K. Prior to each adsorption experiment, the samples were degassed for 12 h at 120 ^oC. The circulator was used to keep the temperature constant during adsorption analysis. Isosteric heats of adsorption (Q_{st}) values were calculated by using the standard calculation routine, which is the Clausius-Clapeyron equation, in the data master offline data reduction software

(Micrometrics). The CO_2/N_2 selectivitity by initial slope method was estimated from the ratio of the initial slopes in the Henry region of the adsorption isotherms. The CO_2/N_2 selectivity by Ideal Adsorbed Solution Theory (IAST) was calculated as follows:

The pure component isotherms of CO_2 measured at 273 and 298 K were fitted with the single-site Langmuir (SSL) model:

$$q_i = q_{i,sat} \times \frac{b_i p_i}{1 + b_i p_i}$$

Where, b_i is the parameter in the pure component Langmuir isotherm (Pa^{-1}), p_i is bulk gas phase pressure of species i (Pa), p_t is total bulk gas phase pressure of mixture (Pa), q_i is molar loading of species i (mol kg^{-1}), $q_{i,sat}$ is saturation capacity of species i (mol kg^{-1}). Pure component isotherm fitting parameters were then used for calculating IAST binary gas adsorption selectivities, S_{ads}, defined as:

$$S_{ads} = \frac{q_1/q_2}{p_1/p_2}$$

The IAST calculations were carried out for binary mixture containing 15 % CO_2 and 85 % N_2, which is typical of flue gases.

Synthetic Section

Synthesis of 9,9',9''-(pyridine-2,4,6-triyl)tris(9H-carbazole) (2,4,6-CzPy)[1]: A mixture of 2,4,6-trifluoropyridine (350 mg, 2.6 mmol), carbazole (1.44 g, 8.6 mmol) and K_2CO_3 (3.3 g, 23.4 mmol) in dimethyl sulfoxide (DMSO) (10 mL) was stirred at 150 ^oC for 12 h under argon atmosphere. After cooling to room temperature, the mixture was poured into water, filtered, and then purified by column chromatography over silica gel with trichloromethane/petroleum as the eluent to afford a white solid. Yield: 90 %. The ^1H NMR spectrum of 2,4,6-CzPy was shown in Fig. S10.

Synthesis of Task-Specific Porous P-PCz: Under argon protection, 2,4,6-CzPy (57 mg, 0.1 mmol) was dissolved in anhydrous dichloromethane (9 mL). The solution was subsequently added dropwise to a mixture of anhydrous $FeCl_3$ (286 mg, 1.76 mmol) and anhydrous dichloromethane (11.8 mL). The resulting mixture was kept stirring under Ar gas flow for 24 h at room temperature. Methanol (20 mL) was then added and stirred for another 1 h to quench the reaction. The obtained polymer was washed with 30 % ammonium hydroxide for 1 h, filtered and washed with water and methanol. The solid was further

purified using Soxhelet extraction with methanol for 24 h and then with tetrahydrofuran for another 24 h. Finally, the desired polymer was collected and dried in a vacuum oven at 80 ^{o}C overnight. Yield: 96 %.

Figures:

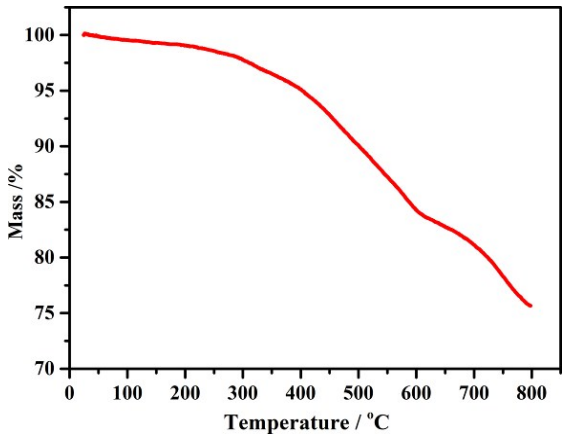

Fig. S1. Thermogravimetric analysis of **P-PCz**.

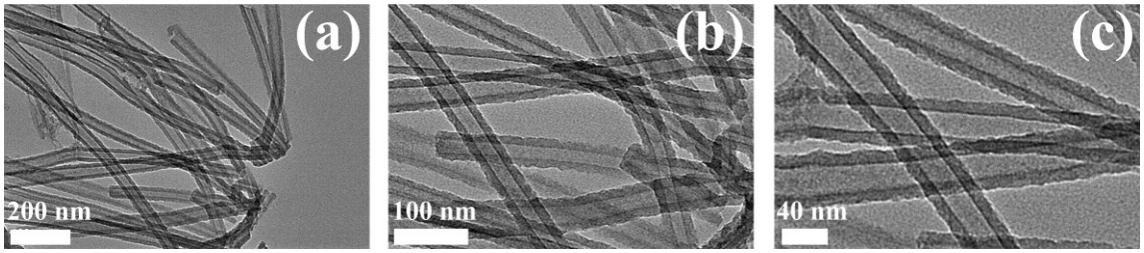

Fig. S2. TEM images of **P-PCz**.

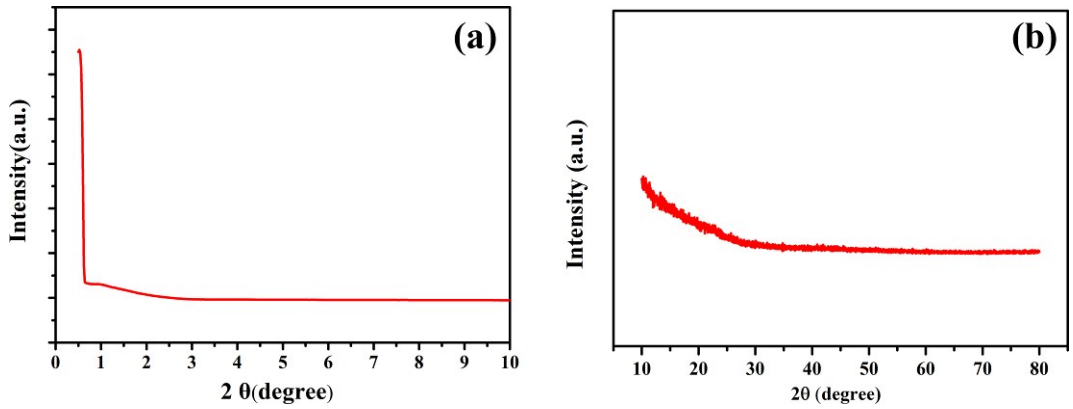

Fig. S3. Low-angle (a) and wide-angle (b) XRD patterns of **P-PCz**.

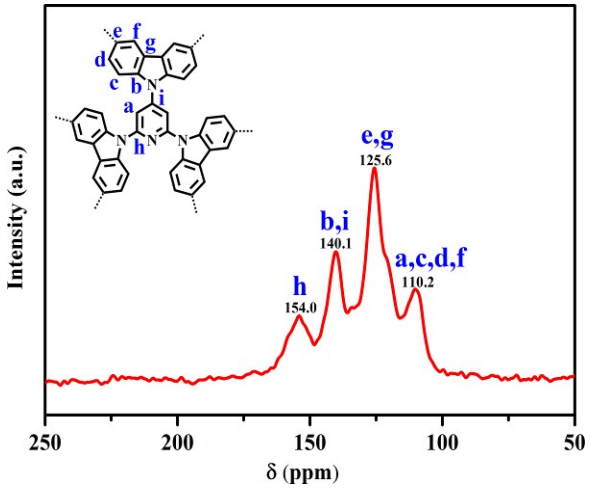

Fig. S4. $^{1}H \rightarrow ^{13}C$ CP/MAS NMR spectra of **P-PCz**.

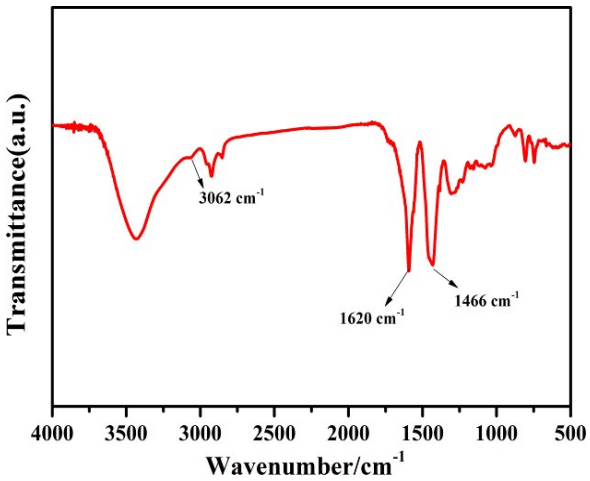

Fig. S5. FT-IR spectrum of **P-PCz**.

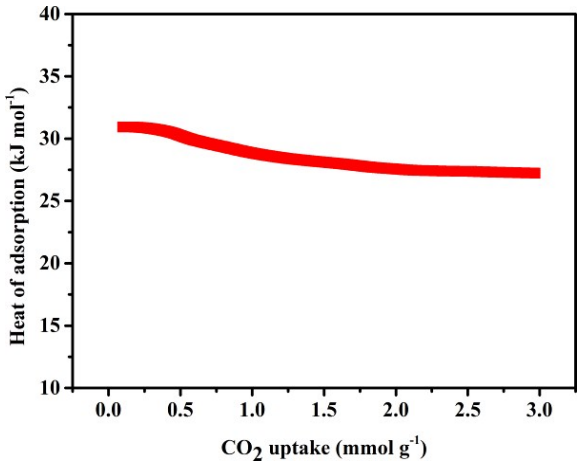

Fig. S6. The isosteric heat of adsorption for **P-PCz**.

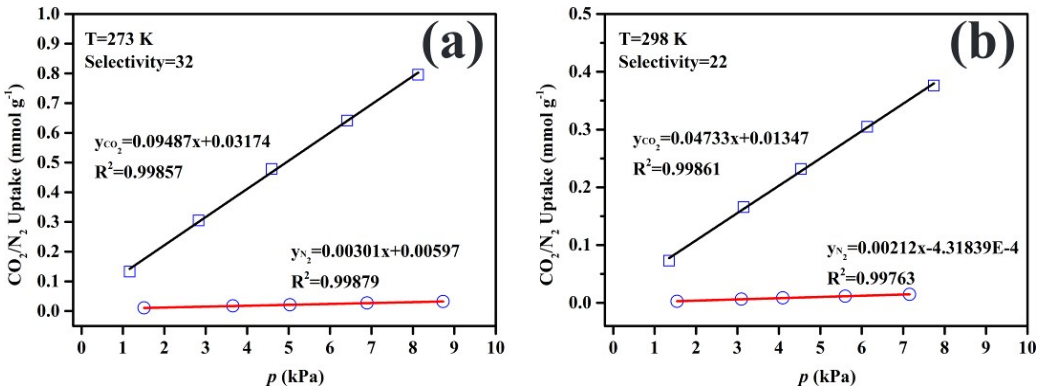

Fig. S7. The selectivity of **P-PCz** for CO_2 over N_2 isotherms obtained from the initial slope method at 273 K (a) and 298 K (b), respectively.

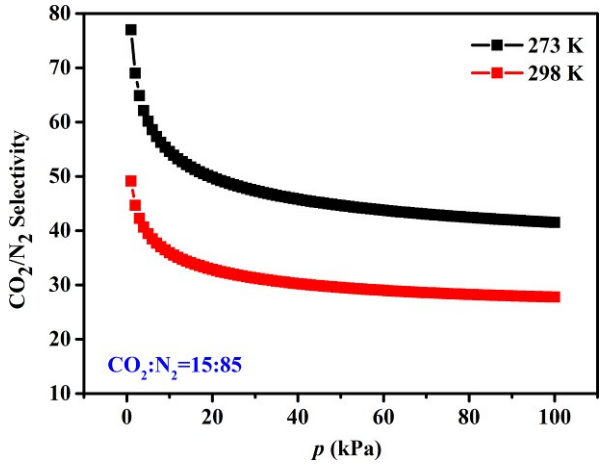

Fig. S8. The selectivity of **P-PCz** for CO_2 over N_2 isotherms obtained from the IAST method at 273 K and 298 K, respectively.

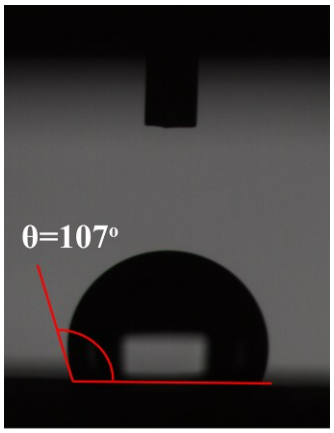

Fig. S9. Digital photograph of **P-PCz** after a drop of water was placed onto the sample.

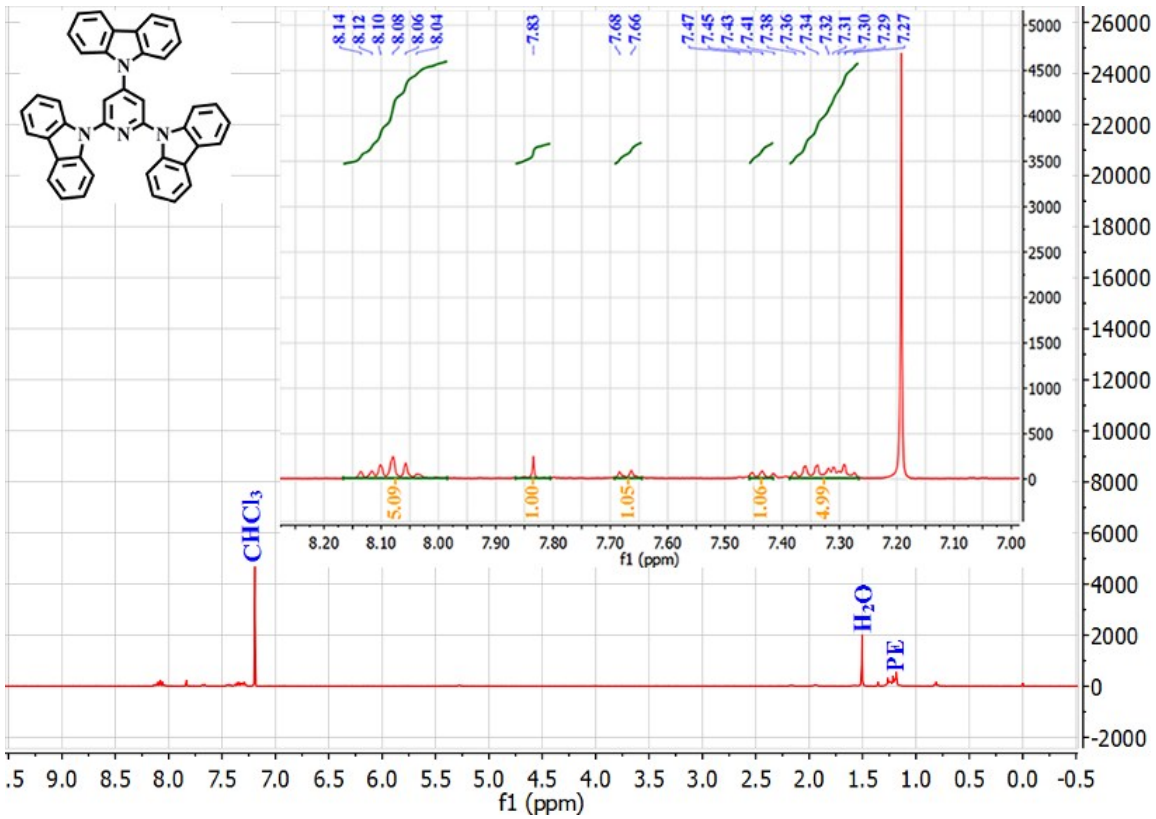

Fig. S10. [1]HNMR spectrum of 2,4,6-CzPy.

Table S1. Summary of surface area, CO_2 uptake, and selectivity (CO_2/N_2) at 273 K in selected POPs.

Adsorbents	BET surface area (m^2/g)	CO_2 uptake (mmol/g)	Selectivity by initial slope method	Ref
P-PCz	**1647**	**5.57**	**32**	**This work**
CPOP-1	2220	4.82	25	2
CPOP-2	510	1.77	–[a]	3
CPOP-3	630	1.91	–	3
CPOP-4	660	2.05	–	3
CPOP-5	1050	2.68	–	3
CPOP-6	980	2.61	–	3
CPOP-7	1430	3.00	30 (ideal)	3
CPOP-8	1610	3.75	–	4
CPOP-9	2440	4.14	–	4
CPOP-10	1110	3.36	–	4
Cz-POP-1	2065	4.59	19	5
Cz-POP-2	671	1.75	26	5
Cz-POP-3	1927	4.77	23	5
Cz-POP-4	914	2.75	37	5
Py-1	437	2.70	117	6
azo-COP-2	729	2.56	109.6	7
ALP-1	1235	5.37	35	8
FCTF-1-600	1535	5.53	19 (IAST)	9
TSP-1	562.5	3.0	32	10
TSP-2	913.0	4.1	38	10
bipy-CTF600	2479	5.58	37	11
BILP-4	1135	5.34	79	12

[a] not determined

Reference:

(1) Tang, C.; Bi, R.; Tao, Y.; Wang, F.; Cao, X.; Wang, S.; Jiang, T.; Zhong, C.; Zhang, H.; Huang, W. *Chem. Commun*. 2015, **51**, 1650.

(2) Chen, Q.; Luo, M.; Hammershøj, P.; Zhou, D.; Han, Y.; Laursen, B. W.; Yan, C.-G. Han, B.-H., *J. Am. Chem. Soc.*, 2012, **134**, 6084.

(3) Chen, Q.; Liu, D.-P.; Luo, M.; Feng, L.-J.; Zhao, Y.-C. Han, B.-H., *Small*, 2014, **10**, 308.

(4) Chen, Q.; Liu, D.-P.; Zhu, J.-H. Han, B.-H., *Macromolecules*, 2014, **47**, 5926.

(5) Zhang, X.; Lu, J. Zhang, J., *Chem. Mater.*, 2014, **26**, 4023.

(6) Luo, Y.; Li, B.; Wang, W.; Wu, K. Tan, B., *Adv. Mater.*, 2012, **24**, 5703.

(7) Patel, H. A.; Je, S. H.; Park, J.; Chen, D. P.; Jung, Y.; Yavuz, C. T. Coskun, A., *Nat. Commun.*, 2013, **4**, 1357.

(8) Arab, P.; Rabbani, M. G.; Sekizkardes, A. K.; İslamoğlu, T. El-Kaderi, H. M., *Chem. Mater.*, 2014, **26**, 1385.

(9) Zhao, Y.; Yao, K. X.; Teng, B.; Zhang, T. Han, Y., *Energy Environ. Sci.*, 2013, **6**, 3684.

(10) Zhu, X.; Mahurin, S. M.; An, S.-H.; Do-Thanh, C.-L.; Tian, C.; Li, Y.; Gill, L. W.; Hagaman, E. W.; Bian, Z.; Zhou, J.-H.; Hu, J.; Liu, H. Dai, S., *Chem. Commun.*, 2014, **50**, 7933.

(11) S. Hug, L. Stegbauer, H. Oh, M. Hirscher and B. V. Lotsch, *Chem. Mater.*, 2015, **27**, 8001

(12) Rabbani, M. G.; El-Kaderi, H. M., *Chem. Mater.*, 2012, **24**, 1511.